錐体細胞の数学的モデルの構築

Mathematical Modeling of Retinal cones

精密工学専攻　43号 Martinecz Antal

1 INTRODUCTION

Vertebrate vision is still superior to the current technology, this can come from different sources: faster computation speed (brain), superior information processing algorithms (brain, retina), better hardware (eyes), etc. As step toward improving our understanding why it is better, this thesis investigates how the signal is formed by the rods and cones of the retina as a reaction to light and what it means from a signal processing perspective.

According to my results, the first part of the cone's signal forming can be characterized as an approximation to a fractional integral. This behavior does not disappear in the subsequent image processing steps and directly affects the output of the cell. As a signal processing step, this provides noise reduction and improves adaptation abilities. Moreover, these findings have also lead to a novel approximation method for the fractional integral.

The second part of the cone's signal forming can be characterized as a nonlinear, slightly underdamped second-order system, with only one overshoot. There might be various reasons for this, it is possible however, that this plays a role in how the signal propagates within the retina. This signals propagation is determined by the frequency characteristics of the subsequent cells have different properties, therefore different frequency components of the signal might be processed differently.

2 THEORETICAL BACKGROUND

2.1 Fractional calculus

2.1.1 Definition

Fractional calculus is a generalization of "traditional" calculus, the same way as real and complex numbers are generalizations of integers. This means, for example, that it is possible to integrate a function real or complex number of times. The fractional integral has multiple, different definitions, one of which is the Riemann-Liouville definition:

$$\mathrm{I}^{\alpha} f(x) = \frac{1}{\Gamma(\alpha)} \int_a^x f(t)(x-t)^{\alpha-1} \mathrm{d}t, \qquad (1)$$

where the $\Gamma(\alpha)$ is the gamma function, the generalization of the factorial function. This can be omitted from the approximation, since in signal processing it only plays a role of a gain.

As an operator, the fractional integral is linear, therefore the response to an impulse (bright flash of light) fully defines its response to any signal. To reflect this property, the Riemann-Liouville definition can be rewritten using convolution [1]:

$$\mathrm{I}^{\alpha} f(x) = \frac{1}{\Gamma(\alpha)} f(t) \otimes t^{\alpha-1}, \qquad (2)$$

which emphasizes, that impulse response of the fractional integral is

$$h(t) = \frac{1}{\Gamma(\alpha)} t^{\alpha-1}. \qquad (3)$$

2.1.2 Interpretation

This paper works with fractional integrals of an order between 0 and 1. In case of these orders, during the course of integration of a signal, more recent values get higher weights (given by $t^{\alpha-1}$), which can be interpreted as signal's past values are gradually forgotten [2].

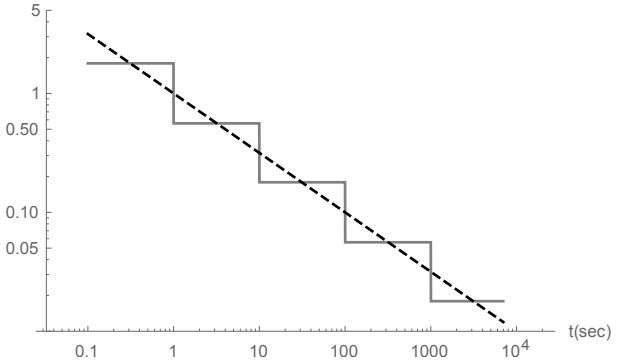

Fig. 1: Piecewise approximation (solid lines) of $f(t) = t^{-0.5}$ (dashed) on a log–log plot.

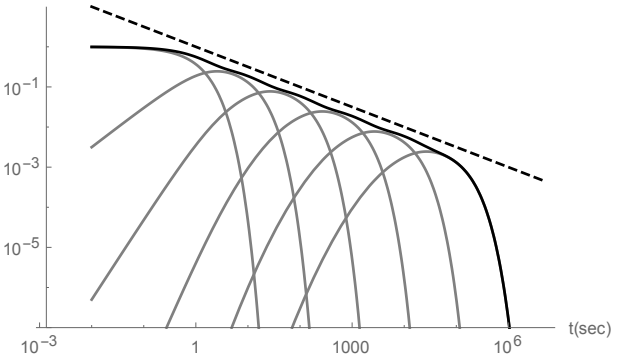

Fig. 2: Approximation of $f(t) = t^{-0.5}$ (dashed) with feedback loops on the log–log plot. Gray lines: contribution of each feedback loop. Black lines: sum of the feedback loops.

2.1.3 Approximation

The linearity property allows approximation by finding a system that approximates the impulse response of the fractional integral, therefore approximating its response to any signal. As it is a power-function, the impulse response is always a straight line on the log–log plot, thus it can be approximated by a piece-wise constant function, see Fig. 1, however it would be inefficient to store all the input values and assign them different weights.

Consecutive feedback loops (also linear), with logarithmically decreasing poles, can be used to store each time interval's data within a single variable. This can be thought of as multiple leaky cups held above one another, with successively smaller holes on their bottom: after pouring water into the top cup multiple times, the levels in each cup can be used to see the signal's history. Similarly to water levels within each cup, internal variables of feedback loops can be used to construct a weighted sum of the signal history. See Fig. 2 for an example.

With differential equations:

$$\dot{x_0} = \text{input}(t) - cx_0 \quad (4a)$$
$$\dot{x_1} = cx_0 - c^2x_1 \quad (4b)$$
$$\dot{x_2} = c^2x_1 - c^3x_2, \quad (4c)$$
$$\vdots$$

where, the output is:

$$y = \sum_i (c^{i(1-\alpha)}x_i), \quad (4d)$$

"c" is the spacing of the feedback loops, optimally $c \approx \frac{1}{10}$.

This approximation is a hybrid between the feedback loop and the fractional integral: on the frequency range of the approximation it behaves as a fractional integral, while on both ends of the frequency range it behaves as a feedback loop, see Fig. 2. The significance of this is that there is always a definite maximum how long signal stays in the system, regardless of how big or long it is, however it can be considerably shorter.

2.2 Cone model

2.2.1 Phototransduction

In rods and cones the signaling starts when a photon hits one of the visual pigments (VPs) thus activating it. As long as they are active, VPs activate their corresponding G-proteins known as "transducins" that are responsible for activating the next step of the signaling. The stages of a VP's activity can be modeled with four feedback-loops:

- freshly activated VPs: with a relative activity of 1 and a pole at ~ 60 1/s,
- phosphorylated VPs: with an activity of 1/64 and a pole at ~ 2.5 1/s,
- arrestin bound VPs: with an activity of 1/640 and a pole at ~ 0.3 1/s,
- inactive VPs, with only spontaneous activity and a pole $\sim 1/30$ 1/s (activity not modeled).

Activate transducins bind to one of the γ subunits of a nearby phosphodiesterase ("PDEs"), which hydrolyze cGMPs as long as the transducin is bound to it. This drops the concentration of cGMPs it within the cells, that causes the closing of the cGMP-gated cation channels in the cell. These channels provide an influx of Ca2+ ions into the cell, while the NCKX transport provides an efflux of Ca2+ from the cell. The rate of this is dependent on the [Ca2+] within the cell. Therefore as a summary, the activation of transducins result in a decrease of [Ca2+] within the cell.

2.2.2 Extension of the Visual Pigments' Mathematical model

For simulations we have extended the model described in[3] with the equations of arrestin bound VPs (Equation 5e):

$$\dot{n_{\text{VP0}}} = \text{input}(t) - \gamma \cdot n_{\text{VP0}} \quad (5a)$$
$$\dot{n_{\text{VP1}}} = \gamma \cdot \text{VP}_0 - (\gamma \cdot 0.9 + 0.5)n_{\text{VP1}} \quad (5b)$$
$$\dot{n_{\text{VP2}}} = \gamma \cdot 0.9n_{\text{VP1}} - (\gamma \cdot 0.9^2 + 1)n_{\text{VP2}} \quad (5c)$$
$$\vdots$$
$$\dot{n_{\text{VP6}}} = \gamma \cdot 0.9^5 n_{\text{VP5}} - 5 \cdot 0.5 n_{\text{VP6}} \quad (5d)$$
$$\dot{n_{\text{VParr}}} = \sum_i (i0.5n_{\text{VPi}}) - 0.3n_{\text{VParr}} \quad (5e)$$
$$\text{VP} = \sum_i (2^{-i}n_{\text{VPi}}) + 2^{-6} \cdot c \cdot n_{\text{VParr}}, \quad (5f)$$

where n_{VPi} is the number of VPs with the phosphorylation level i, and γ is the rate of phosphorylation. "VP" is the sum of the VPs' activities: the number of transducins activated per second. "c" is the inhibition after arrestin binding (c=0.1 for a 90% inhibition).

As these equations describe a fractional integral, the model can be reduced to the following without affecting the output:

$$\dot{n_{\text{VP0}}} = \text{input}(t) - \gamma \cdot 0.9^5 n_{\text{VP0}} \quad (6a)$$
$$\dot{n_{\text{VP6}}} = \gamma \cdot 0.9^5 n_{\text{VP5}} - 2.5n_{\text{VP6}} \quad (6b)$$
$$\dot{n_{\text{arrVP}}} = 2.5 \cdot n_{\text{VP6}} - 0.3n_{\text{arrVP}} \quad (6c)$$
$$\text{VP} = n_{\text{VP0}} + 2^{-6}n_{\text{VP6}} + 2^{-6} \cdot c \cdot n_{\text{arrVP}}. \quad (6d)$$

Extending the full cone model of[3] with arrestin bound VPs increases the fit to the experimental data, however it decreases the fit from the steady state values. This deviation from the steady state values was also mentioned in[3], where it was fitted by allowing one of the poles to decrease with time as an adaptation. While this is omitted from our simulations, it implies that there might be an adaptive process that can make the steady-state values constant.

As more and more VPs are in an active or deactivated state, there is less and less chance of a photon actually hitting a default state VP. This can be modeled as decreasing the input sensitivity for each missing VP:

$$\text{input}^*(\text{t}) = \text{input}(\text{t}) \cdot (1 - \frac{n_{\text{VPused}}}{n_{\text{VPall}}}), \quad (7)$$

where $n_{\text{VPall}} = 10^7$ as reported by Lamb[4].

However VPs are recycled in the retinal pigment epithelium, a row of cells behind the photoreceptors, each of these cells actually regenerate multiple cone's VPs. Therefore this model is cumbersome to use for multiple photoreceptors (in a video), as they affect each other, the differential equations cannot be calculated independently for each pixel. Furthermore, cones have two sources of VP regeneration one is the same as rods, the other is just for cones[5], this however is omitted from my model.

For computation on videos, the retinoid cycle can be approximated as a separate pre-processing step for the whole video. In this case, all the used VPs can be computed separately with one feedback loop, blurring each image frame to imitate the effect of neighboring cones affecting each other.

3 RESULTS AND DISCUSSION

3.1 Bode Plots

Bode-plots fully define a linear system's behavior, they describe the relationship between the input's frequency and the output's phase and amplification. For a fractional integral (I^α), the phase shift is constant at -90α degrees and the amplification has a slope of -20α dB/dec[6]. This is achieved by the approximation which provides a further proof that it is indeed a proper approximation.

The VPs activity approximate the fractional integral, as seen on Fig. 3. The quality of this approximation mainly depends on the relative activities of different stages: with most of the published activities it fits the approximation.

When compared to a feedback loop, the fractional integral's constant phase shift of -90α degrees could alter the perception of patterns or position of moving objects, however we have failed to show any deviation from it (that originates from the phase).

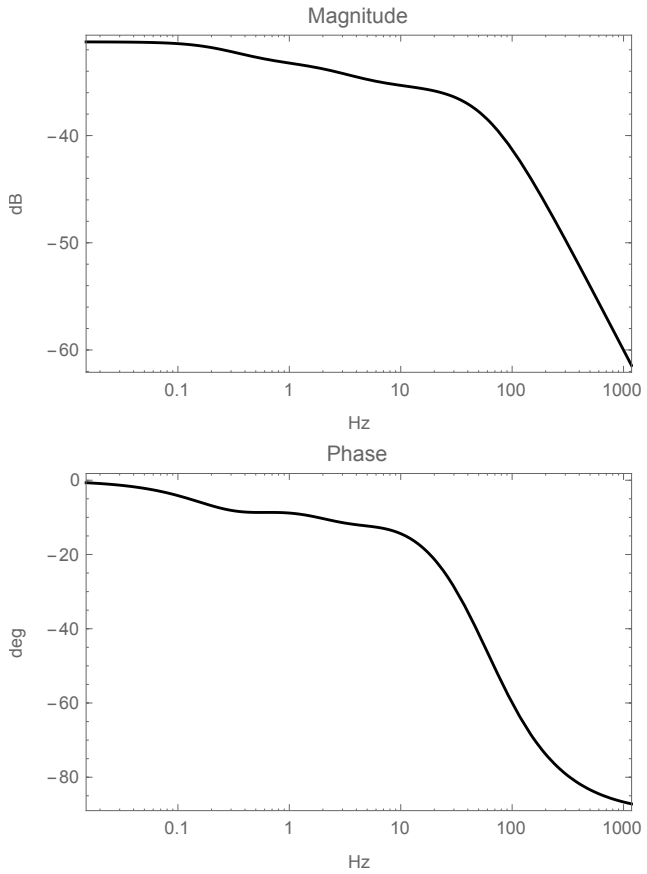

Fig. 3: Bode-plots of the VPs activity, where the inhibition of ArrVPs is 90%.

Fig. 4: Effects of the fractional integral on a moving object (from left to right): Top: effects of a fast feedback loop. Middle: effect of a slow feedback loop. Bottom: Weighted sum of the top and middle images: approximation of fractional integral $I^{0.2}$, the same as the VPs activity.

3.2 Noise reduction and movement

According to my results, the approximation of a fractional integral in signal processing reduces noise. When compared to a first-order feedback loop, this noise reduction, it is a lot more subtle, however affects signals on wider frequency ranges. Therefore it is possible to retain some of the high-frequency data: fast moving objects are not disappear or are not blurred. The fractional integrals noise suppressing ability can be seen, for example, during snowfall: it is important to be aware of the phenomena, however individual snowflakes should be suppressed as long as we are not focusing on them. In case of a first order filter, the snowflakes might completely disappear or are unaffected depending on their speed. See Fig. 4 on how the response is built.

3.3 Adaptation

Adaptive processes can benefit from this behavior: higher input ranges can only be achieved by sustained strong inputs, as the maximal input is constrained by the pupils and the "charging" of residual activities take time. Therefore it is possible to differentiate between light conditions and input signals. Similar conclusions were drawn in [7], where the adaptation of auditory-nerve model was extended by similar power-law components.

3.4 Deviations from the approximation

If in Equation 6d the arrestin-bound VP's activity is a biological constraint (achieving a perfect shut-of is difficult), the possible values of VP6 activity can be put into three categories, it can be:

- just right for the approximation (the experimental values),
- too high for the approximation ($\sim 400\%$ of the experimental),
- too low for the approximation ($\sim 10\%$ of the experimental).

If it is too high, the feedback-loop's pole dominates the response making it sluggish. If it is too slow then on off part of the signal, there will be a residual activity (afterimage) that does not fade well. See Fig. 5 for comparison.

Through the slow settling of step responses, the fractional integral also affects the the size of the overshoots and the speed of the next processing steps. In this case the approximation seems to be an acceptable trade-off between speed and accuracy, see Fig. 6.

3.5 Short-Term Visual Memory

Afterimages can used as a short-term visual memory; this phenomena is stronger in rods than cones [8]. This is consistent with our results: in rods the slow phosphorylation is the source of afterimages; while in cones only the residual activities are the sources of afterimages.

3.6 Eye movements

Eye movements play a special role in image processing by choosing and changing focus a few times per second. Focus makes the objects of interests to be projected on the same spot on the retina (fovea), therefore a series of static images that change with a few Hz are processed instead of a moving image. In relation to this, it might play a role, that the neurons responsible for stabilizing eye movements also show a fractional integral-like behavior [9].

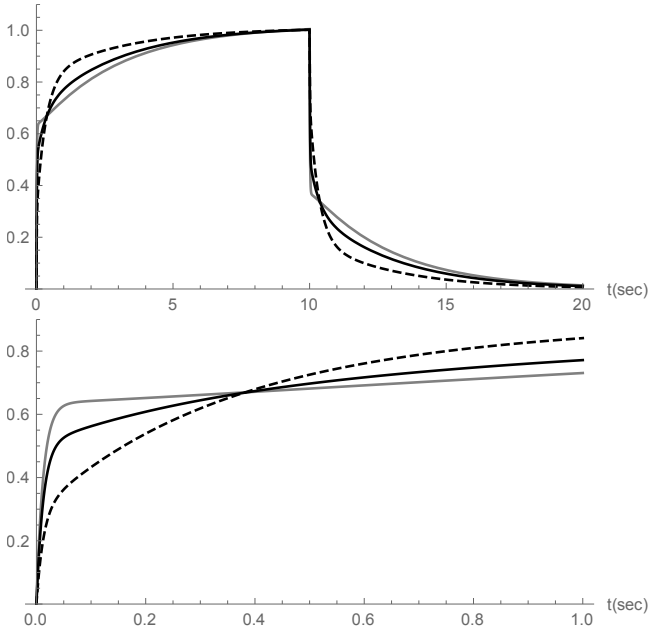

Fig. 5: Normalized 10 sec. step-responses of different VP activities: fractional integrals and deviations from it. Black line: fractional integral. Grey: low VP6 activity. Dashed: strong VP6 activity. The top and bottom images are the same step response, but plotted on different timescales. The y-axis is the relative activity of VPs (dimensionless).

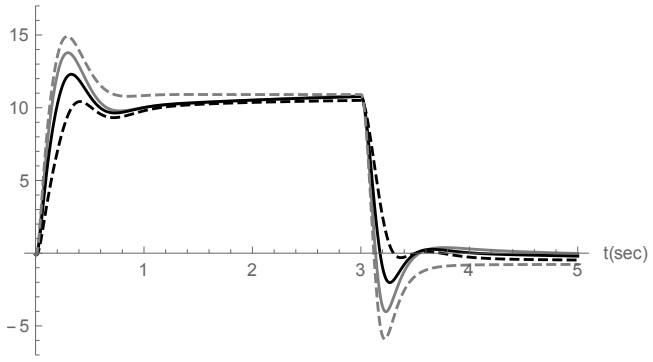

Fig. 6: Responses of the full model described in [3]. Normalized, 10 sec. step-responses of different VP activities: fractional integrals and deviations from it. Black line: fractional integral. Grey: low VP6 activity. Dashed: strong VP6 activity. Dashed gray: no residual activities (original model).

3.7 Neighboring cells and frequency ranges

The subsequent cells in processing are either low-pass or band pass (high-pass with biological constraints) [10,11]. The cones' response can also be divided into two similar groups: high frequency (overshoots) and low frequency (steady state) parts. The significance of this distinction is that the sizes of the overshoots are unaffected by the adaptive processes, and as it is indicative of a derivative component reflect the size of the change in the input signal.

My hypothesis is that low frequency values also act as an internal variable or reference value that can change with the input, while the signal can be reconstructed more accurately using the higher frequency data (at a later stage). For example, when transitioning from a dark area to a brighter area the retinoid cycle adjusts the sensitivity of the cell within a second or so, while it can still be understood how the different colors relate to each other.

3.8 Retinoid cycle

As mentioned before, the temporary "disappearance" of VPs (as they are used up) decreases the sensitivity of the cell. This process only affects the output on longer timescales and across groups of cells, as the adaptation affects higher input ranges more than lower ones. Therefore, a group of different colors (red green and blue) will approach a less saturated (grey) color. This appears as a negative afterimage after changing the input image.

4 CONCLUSIONS

We have shown how residual activities are connected to fractional integrals, how this affect the signaling and its possible advantages. Although the validity of residual activities in modeling seem to be supported by biological data, it introduces new questions (steady state values should remain constant), therefore the topic requires further investigation.

References

(1) I. Podlubny, "Fractional-Order Systems and PID controllers," vol. **44**, no. 1, pp. 208–214, (1999).

(2) I. Podlubny, "Geometric and Physical Interpretation of Fractional Integration and Fractional Differentiation," *Fractional Calculus and Applied Analysis*, vol. **5**, pp. 367–386, (2002).

(3) J. I. Korenbrot, "Speed, adaptation, and stability of the response to light in cone photoreceptors: The functional role of Ca-dependent modulation of ligand sensitivity in cGMP-gated ion channels," *The Journal of General Physiology*, vol. **139**, pp. 31–56, (2012).

(4) T. D. Lamb and E. N. Pugh, "Dark adaptation and the retinoid cycle of vision.," *Progress in retinal and eye research*, vol. **23**, pp. 307–80, (2004).

(5) J. S. Wang and V. J. Kefalov, "The Cone-specific visual cycle," (2011).

(6) B. Vinagre, I. Podlubny, A. Hernandez, and V. Feliu, "Some approximations of fractional order operators used in control theory and applications," *Fractional Calculus and Applied Analysis*, vol. **3**, no. 3, (2000).

(7) M. S. a. Zilany and L. H. Carney, "Power-law dynamics in an auditory-nerve model can account for neural adaptation to sound-level statistics.," *The Journal of neuroscience*, vol. **30**, pp. 10380–90, (2010).

(8) I. G. Sligte, H. S. Scholte, and V. a. F. Lamme, "Are there multiple visual short-term memory stores?," *PloS one*, vol. **3**, p. e1699, (2008).

(9) T. J. Anastasio, "The fractional-order dynamics of brainstem vestibulo-oculomotor neurons.," *Biological cybernetics*, vol. **72**, pp. 69–79, (1994).

(10) W. Bialek and W. G. Owen, "Temporal filtering in retinal bipolar cells. Elements of an optimal computation?," *Biophysical journal*, vol. **58**, no. 5, pp. 1227–1233, (1990).

(11) T. Euler, S. Haverkamp, T. Schubert, and T. Baden, "Retinal bipolar cells : Elementary building blocks of vision," *Nature Publishing Group*, vol. **15**, no. 8, pp. 507–519, (2014).